schematically in Fig. 2. Measurements of such temperature-dependent effects would also give the temperature dependence of the effective droplet surface tension and perhaps clarify whether this droplet surface tension is approximated better by the bulk surface tension used in this paper or by the "microscopic" surface tension used in Ref. 1 (see also Binder *et al.*[12] and Frisch[5]).

We conclude that Fisher's droplet picture basically reconfirms the results of the classical homogeneous and heterogeneous nucleation theory[2] near 0 °C; near the critical point, our correction factors Z_1 and Z_2 make the nucleation rates much smaller. We suggest to measure the nucleation rates over a larger temperature interval in order to determine the effective droplet surface tension and to check our result (Fig. 2) that near T_c the homogeneous nucleation rates dominates the heterogeneous one. A more detailed report is available upon request.

We thank Dr. K. C. Russel for his comments, and one of us (C.S.K.) is grateful to the Advanced Study Program, National Center for Atmospheric Research, Boulder, Colorado, for its hospitality.

*Address until Sept. 1, 1972: Department of Physics, University of Illinois, Urbana, Ill.; work supported by NSF Grant No. GP-16886.

†Work partially supported by NSF Grant No. GA-33422 and Research Corporation, Fredrick Gardner Cottrell Grant aid. Reprint request to C. S. Kiang.

‡Present address: Institute Laue-Langevin, 8046 Garching, W. Germany.

[1]Clark College Research Group (C. S. Kiang *et al.*), J. Atmospheric Sci. 28, 1222 (1971).

[2]N. H. Fletcher, *The Physics of Rainclouds* (Cambridge U. P., Cambridge, England 1966), Chap. III.

[3]K. C. Russell, J. Chem. Phys. 50, 1809 (1969).

[4]J. Feder, K. C. Russell, J. Lothe, and G. M. Pound, Advan. Phys. 15, 117 (1966).

[5]International Workshop on Nucleation Theory and Its Applications, Clark College, Atlanta, 1972 (unpublished) (abstracts available), organized by C. S. Kiang.

[6]M. E. Fisher, Physics 3, 225 (1967).

[7]J. L. Katz and B. J. Ostermier, J. Chem. Phys. 47, 478 (1967).

[8]Clark College Research Group (D. Stauffer *et al.*), Chem. Phys. Letters (to be published).

[9]C. S. Kiang and D. Stauffer, Z. Physik 235, 130 (1970).

[10]W. Rathjen, D. Stauffer, and C. S. Kiang, Phys. Letters (to be published).

[11]L. Krastanow, Z. Meteorol. 58, 37 (1941).

[12]K. Binder and D. Stauffer, J. Statistical Phys. 6, 49 (1972); E. Stoll, K. Binder, and T. Schneider, preceding paper, Phys. Rev. B 6, 2777 (1972).

PHYSICAL REVIEW B VOLUME 6, NUMBER 7 1 OCTOBER 1972

Exchange Narrowing of Fine Structure in Dilute Magnetic Alloys: Mg : Gd†

P. H. Zimmermann, D. Davidov, R. Orbach, L. J. Tao, and J. Zitkova
Department of Physics, University of California, Los Angeles, California 90024

(Received 1 May 1972)

The magnetic-resonance spectrum of dilute Mg:Gd alloys is analyzed using the full coupled localized-conduction-electron transverse-susceptibility expression derived by Barnes. An analysis of the significance of the individual terms in the susceptibility matrix is presented, along with a physical interpretation of exchange narrowing of fine-structure splittings in dilute magnetic alloys. A value of $D = 140$ G for the fine-structure parameter is extracted from a fit to the theory. Comparison is made with a moment analysis utilized previously.

I. INTRODUCTION

Previously,[1] we reported the anisotropic magnetic-resonance spectrum of dilute single-crystal Mg : Gd alloys (referred to in the following as I). We attributed the temperature and angular shifts of the field for resonance to *unresolved* fine structure. Using the method of moments, we extracted a fine-structure parameter $D = 155$ G and an (isotropic) g factor of 1.98. Our moment analysis of the linewidth was not satisfactory; the magnitude scaled correctly with the angle, but was nearly an order of magnitude larger than what was observed. We speculated that this discrepancy was caused by a magnetic-resonance bottleneck, leading to an exchange narrowing of the fine-structure-split line. After our paper appeared, we did observe[2] *resolved* fine structure in another dilute single-crystal alloy, Au : Gd. We developed a theory for the exchange narrowing of fine structure in this alloy. The method was limited to alloys in the absence of a magnetic-resonance bottleneck and was applicable to Au : Gd because of the large contrast between the host and (rare-earth) impurity spin-orbit coupling.[3] We also included a crude form of spin-spin interaction.

However, as discussed in I, Mg : Gd is almost certainly bottlenecked. Using the value of the

exchange-coupling constant J extracted from linewidth measurements of Burr and Orbach[4] on (unbottlenecked) Mg : Er, one expects an increase in the resonance linewidth of Mg : Gd of 150 G/deg at $\theta = 55°$ (θ is the angle between the c axis and the magnetic field), where the fine structure collapses. Instead, we measure 12 G/deg. The discrepancy was attributed to a partial magnetic-resonance bottleneck in I. Recently, Barnes,[5] using a diagrammatic method developed by himself and Zitkova,[6] developed a full theory for the dynamic transverse susceptibility of a dilute magnetic alloy, including fine structure and the coupled response of the localized and conduction electrons. The purpose of this paper is to apply his results to our measurements on Mg : Gd as reported in I.

In Sec. II we discuss some of the physical content contained in Barnes's theory. His full expression for the dynamic susceptibility is fitted to our experimental spectra in Sec. III. A discussion is given of the sensitivity of the fit to changes in the parameters, and a comparison is made with our previous moment analysis. We also point out a possible method for the determination of the actual spin-spin "field" distribution in a dilute alloy from an analysis of partially resolved magnetic-resonance fine structure in the intermediate-narrowing regime.

II. DYNAMIC-SUSCEPTIBILITY ANALYSIS

The result of Barnes[5] for the dynamic coupled magnetic susceptibility of an alloy, including fine structure, is reproduced in the Appendix. When the lattice damping is sufficiently large to break the magnetic-resonance bottleneck, his response function should reduce to that of Ref. 2. Before actually carrying out the detailed fit to Barnes's theory, we discuss some of the physical consequences of his result. We first note that, even in the absence of a magnetic-resonance bottleneck, exchange narrowing of fine-structure-split lines can occur. This is illustrated in Fig. 1, where hypothetical fine-structure-split spectra are displayed for various values of the localized-conduction-electron exchange parameter J. The various contributions are as follows.

A. Longitudinal Fluctuations

Each fine-structure line is broadened by longitudinal fluctuations of the conduction-electron spin. In conventional terminology, the contribution to the linewidth is equal to

$$1/T_2' = 2\pi(\rho J)^2 kT. \qquad (1)$$

Here, ρ is the conduction-electron one-spin density of states at the Fermi energy and J is the exchange integral defined by $2J\,\vec{S}\cdot\vec{s}$, where $\vec{S}$ is the spin of the magnetic impurity and $\vec{s}$ is the spin of the conduction electrons. Though it may not seem obvious, (1) represents the longitudinal scattering-out contribution from the localized spin-resonance line to the conduction-electron spin-resonance line. This is demonstrated explicitly in Ref. 6.

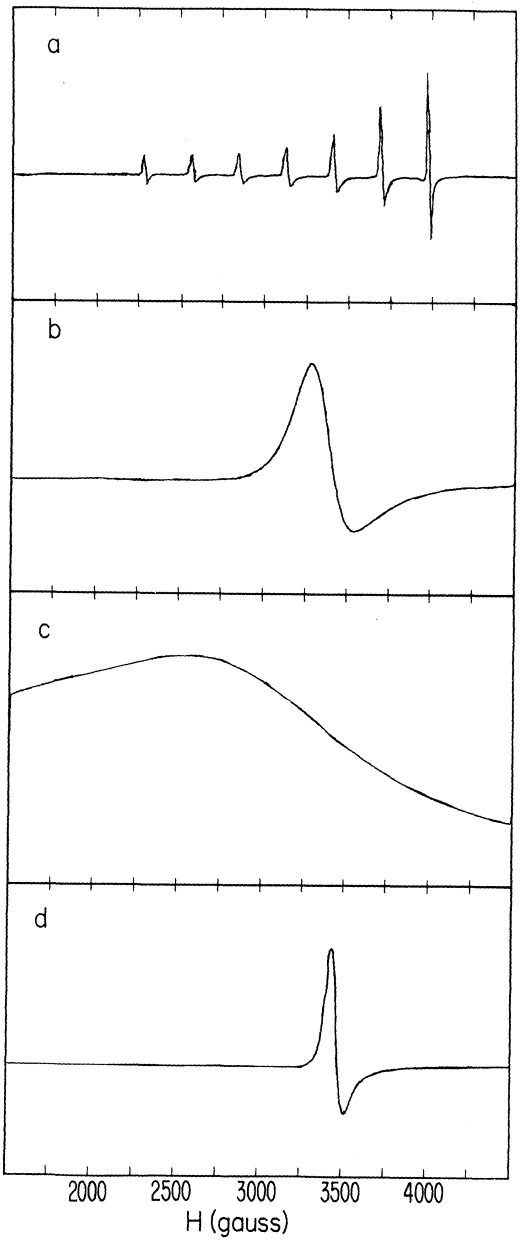

FIG. 1. (a) Resonance spectrum for $S=\frac{7}{2}$, $D=140$ G, $T=1.4$ °K. Large lattice damping of the conduction-electron spins is present, and a nominal exchange $J=0.015$ eV is used, so that no bottleneck is present. (b) Same as (a), but $J=0.2$ eV, the value appropriate to Mg : Gd (see text). (c) Same as (b), but scattering-in terms have been omitted from the response matrix. (d) Same as (b), but with no lattice damping of the conduction-electron spins so that an extreme bottleneck is present.

B. Transverse Fluctuations

At small J, we can discuss the structure of the individual fine-structure lines. The transverse fluctuations of the conduction electrons contribute to the linewidth of the transition $S^z \leftrightarrow S^z+1$ an amount equal to

$$1/T_1' = \pi(\rho J)^2 kT\{[S(S+1)-(S^z+1)(S^z+2)] + 2[S(S+1)-S^z(S^z+1)]+[S(S+1)-S^z(S^z-1)]\}. \quad (2)$$

The second square-bracketed term in (2) arises from exchange-induced transitions between the states S^z and S^z+1, while the first and third arise from exchange-induced lifetime-broadening transitions between states S^z+1 and S^z+2, and S^z-1 and S^z, respectively.

The contribution of (2) can also be thought of as a "scattering-out" contribution to the linewidth, but to a number of resonance lines as well as the conduction electrons. In a matrix representation of the response function, where the rows and columns are labeled by the localized and conduction-electron transition energies (an 8×8 for Mg : Gd, composed of $2S=7$ fine-structure lines and the conduction-electron line), Eqs. (1) and (2) will be found on the diagonal. Then (2) represents the diagonal scattering-out rate to the two neighboring fine-structure and the conduction-electron transitions. This can be seen by rewriting (2) as

$$1/T_1' = 2\pi(\rho J)^2 kT\{[S(S+1)-(S^z+1)(S^z+2)] + [S(S+1)-S^z(S^z-1)]\}+2\pi(\rho J)^2 kT. \quad (3)$$

The two terms in the curly brackets of the equation represent the rate of "scattering out to other fine-structure lines"— in this instance those two spin-resonance lines corresponding to the transitions $S^z-1 \leftrightarrow S^z$ and $S^z+1 \leftrightarrow S^z+2$. The second term represents a contribution to the linewidth of the $S^z \leftrightarrow S^z+1$ transition line from scattering out to the conduction-electron spin. Comparison with (1) demonstrates the equality of this contribution with that arising from longitudinal fluctuations, a point first made by Zitkova *et al.*[7] It will turn out (see below) that scattering-in terms from the adjacent fine-structure transitions will cancel the first but not the second term in (3), if J is sufficiently large such that the sum of Eqs. (1) and (2) exceeds the fine-structure splitting. We will then obtain a linewidth only from scattering-out terms to the conduction electrons. This is seen to be just the Hebel–Slichter[8] result that

$$\frac{1}{T_2} = \frac{1}{T_2'} + \frac{1}{T_1'} = 4\pi(\rho J)^2 kT,$$

independent of S and S^z. This width is substantially narrower than a fine-structure-split spectrum with each line possessing the full scattering-out width. This can be seen by comparing Fig. 1(a) and 1(b). The former exhibits the fine-structure spectrum with parameters appropriate to Mg : Gd (see Sec. II), but for negligible J. The latter represents the fine-structure spectrum with parameters appropriate to Mg : Gd, but with large lattice damping of the conduction electrons so that the magnetic-resonance bottleneck is broken. Full scattering-out terms contain spin-flip rates for $S=\frac{7}{2}$, $S^z=\pm\frac{1}{2}$ transitions which are 16 times that for $S=\frac{1}{2}$, $S^z=\pm\frac{1}{2}$ transitions. (The $S=\frac{1}{2}$ rate equals the fully collapsed Hebel–Slichter rate.)

As Chock *et al.*[2] and Barnes[5] demonstrate, exchange "scattering-in" terms arising from transitions *between* fine-structure lines are also present. These terms are unimportant if the localized spin transition rates are less than the fine-structure splitting $2D$ [Fig. 1(a)]. However, for larger J (or kT), they can become comparable to, or even greater than, $2D$. For the transition $S^z \leftrightarrow S^z+1$, with a total scattering-out linewidth of the sum of Eqs. (1) and (2), the scattering-in terms from adjacent fine-structure transitions equal

$$2\pi(\rho J)^2 kT[S(S+1)-(S^z+1)(S^z+2)], \quad (4a)$$

$$2\pi(\rho J)^2 kT[S(S+1)-S^z(S^z-1)]. \quad (4b)$$

The term (4a) is the scattering-in rate from the fine-structure transition $S^z+1 \leftrightarrow S^z+2$ to the transition $S^z \leftrightarrow S^z+1$, while (4b) is the scattering-in rate from $S^z-1 \leftrightarrow S^z$ to the same transition $S^z \leftrightarrow S^z+1$. In the matrix formulation referred to earlier, these terms would be found in the immediate off-diagonal positions between the fine-structure states they connect. When these rates exceed the difference in the real parts of diagonal energy elements (in this instance, $2D$), collapse occurs and a cancellation between (4) and (3) is obtained. As one passes to the limit of extreme narrowing, this cancellation is complete and, as stated above, all that remains is the uncompensated Hebel–Slichter width

$$1/T_2 = 4\pi(\rho J)^2 kT. \quad (5)$$

To see the effect of this cancellation, Fig. 1(c) exhibits the spectrum if only the scattering-out terms (1) and (2) were kept in the rate equations. We have certainly shown, as claimed in the Introduction, that narrowing occurs in the sense of the fine-structure features being overwhelmed by off-diagonal exchange-induced transition rates [Eq. (4)], yielding the unbottlenecked exchange width independent of spin [Eq. (5)]. The off-diagonal spin-flip matrix elements [Eq. (4)], when very much larger than the difference in diagonal energy matrix elements, destroy the phase dif-

ference provided by the fine-structure splitting, and cancel the scattering-out spin-dependent part of (3). We believe our results[2] for Au : Gd are appropriate to this limit.

If the exchange is increased still further, or the lattice relaxation of the conduction-electron spins is reduced, the regime of the magnetic-resonance bottleneck is reached. The conduction-electron magnetization is locked in-phase to the localized spin magnetization and provides a magnetization scattering-in rate of $(g_s/g_e)(\chi_e/T_{es})$, where χ_e is the conduction-electron static susceptibility, and $1/T_{es}=\frac{8}{3}\pi\rho J^2 S(S+1)$ is the Overhauser[9] rate, ρ being the one-spin conduction-electron density of states. The collapsed fine-structure magnetization scattering-out rate is χ_s/T_{se}, where χ_s is the static susceptibility of the localized spins, and $1/T_{se}$ the Hebel–Slichter rate [Eq. (5)]. For equal g factors, these rates are equal, and the collapsed fine-structure line is then further narrowed to the conventional bottleneck limit, as displayed in Fig. 1(d). The remaining width originates from residual broadenings, of magnitude D^2T_2, and the usual bottleneck width[10] arising from lattice relaxation of the conduction-electron spin. We believe our results in I are appropriate to this limit.

There is another interesting, but yet unexplored, regime. This arises from the possibility of bottlenecking each of the fine-structure lines separately. It occurs when the scattering-out rate [the sum of Eqs. (1) and (2)] is less than the fine-structure splitting $2D$, but the exchange conduction-electron to localized spin (Overhauser) rate is sufficiently strong to create bottleneck conditions. This also requires small lattice relaxation of the conduction-electron spin. The regime is equivalent to limit B of the analogous situation for hyperfine splitting in a dilute magnetic alloy, as discussed by Barnes *et al.*[11] The full fine-structure splittings occur, but each resolved line possesses a width equal to the sum of Eqs. (1) and (3), but with the factor $1/T_2$ [defined in (5)] replaced by $[(\chi_S^{(0)}-\chi_{S^z}^{(0)})/\chi_S^{(0)}](1/T_2)$. The quantity $\chi_S^{(0)}=\sum\chi_{S^z}^{(0)}$ from $-S<S^z<S-1$, where $\chi_{S^z}^{(0)}$ is defined in the Appendix immediately after (A9). In the high-temperature approximation, this reduction of $1/T_2$ can be rewritten

$$\{[(4S-1)S(S+1)+3S^z(S^z+1)]/[(2S+1)S(S+1)]\}(1/T_2),$$

where S^z labels the lower of the two levels between which the transition is made. For hyperfine splittings,[11] each transition has the same oscillator strength, so that the reduction of the width is the simple factor $[2I/(2I+1)](1/T_2)$. This regime may not be easily accessible, requiring fortuitous ratios of a number of parameters, but its existence should be recognized.

III. EXPERIMENTAL FIT FOR Mg:Gd

It is now of interest to determine which limit is appropriate to the results of Tao *et al.*[1] on Mg : Gd. Angular measurements of the relaxation rate in Mg : Er[12] demonstrate the absence of a magnetic-resonance bottleneck in that system. Linewidth measurements can then yield a value for J, using the results of Orbach and Spencer.[13] The density of conduction-electron states at the Fermi energy for Mg metal, $\rho=0.2$ states/atom spin eV, is obtained from the specific heat.[14] Phonon-mass enhancement is neglected because theoretical estimates[15] indicate that it is small. A Pauli-spin susceptibility of $\chi_e=13\times10^{-6}$ emu/mole, very close to that measured for Mg metal, is obtained from this value of ρ. This means the exchange enhancement of the susceptibility is negligible, so that the correction factor of Moriya[16] can be ignored. We find $J=0.16$ eV for Mg : Er. The fact that Mg : Yb[12] is diamagnetic implies substantial covalent (negative) contributions to the exchange couplings towards the end of the rare-earth series. A slightly larger value of J is expected, therefore, for Mg:Gd than for Mg : Er, because of the greater stability of the $4f$ shell in the former alloy. We choose, therefore, $J=0.2$ eV for Mg : Gd. This would lead to a Hebel–Slichter linewidth of 150 G/deg at $\theta=55°$, where the fine structure collapses and the result (5) is expected to be valid. Experiments[1] exhibit instead an order of magnitude smaller width of only 12 G/deg. This result implies the presence of a magnetic-resonance bottleneck and allows us to obtain a value for the conduction-electron relaxation rate $\Delta_{eL}=10^{10}$ sec^{-1} at the Gd concentration in I of $c=400$ ppm. We also observe a residual width of 100 G at this angle. As one rotates away from 55°, the fine structure broadens the line in a complicated manner (the whole point of this paper), and it proves very difficult to extract an angular dependence of the residual width. For that reason, we shall assume in our final fitting procedure that each fine-structure line is residually broadened by 100 G, independent of angle. We recognize this assumption is very crude. Only with a knowledge of the internal strain distribution and the appropriate four spin-strain coupling coefficients could we improve on this approximation using the method of Feher.[17]

The only remaining unknown parameter in the expression of Barnes is the axial field splitting constant D. As discussed in the Introduction, a value of $D=155$ G was obtained in I with the use of a first-moment fit. The analysis implicitly assumed a symmetric magnetic-resonance line, Lorentzian in shape. However, the exchange and lattice-relaxation rates derived above are such that Mg : Gd lies in the intermediate bottleneck

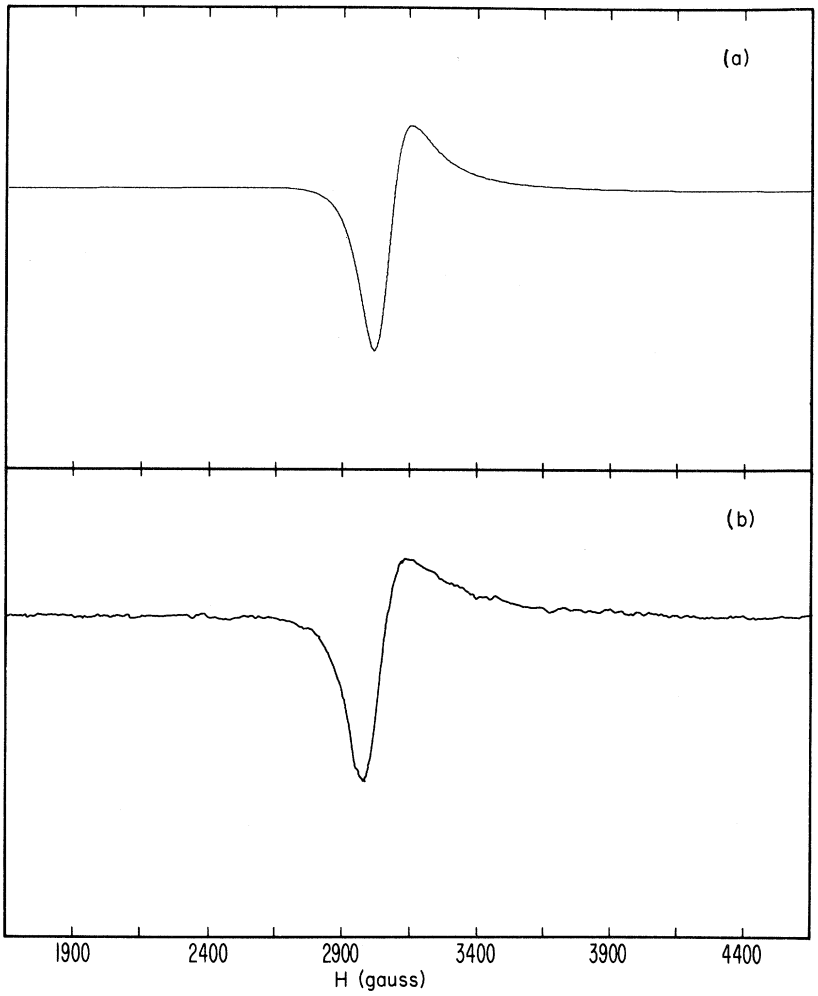

FIG. 2. Theoretical line shape for Mg : Gd, for the angle between the magnetic field and the c axis $\theta = 90°$, and $T = 1.4$ °K. $J = 0.2$ eV, the residual width is taken to be 100 G for each fine-structure line, $D = 140$ G, $\Delta_{eL} = 10^{10}$ sec^{-1}, and $c = 400$ ppm. (b) Experimental magnetic-resonance line for Mg : Gd, at $\theta = 90°$, $T = 1.4$ °K, and at 8.7 GHz.

regime. In this region, the computer-derived magnetic-resonance absorption line shapes are not quite symmetric, making our previous moment analysis somewhat in error. We find a best fit for $D = 140$ G, using the full matrix expression of Barnes.[5] Figure 2(a) illustrates the theoretical line shape obtained at $\theta = 90°$ and $T = 1.4$ °K, along with an example of our magnetic-resonance data at the same angle and temperature, Fig. 2(b). Figure 3 displays the field for resonance and magnetic-resonance linewidth for arbitrary angle, at $T = 1.4$ and 4.2 °K, and at 8.7 and 35 GHz. The dashed line is that which a second-moment analysis of only the fine structure would yield. Comparison with the experimental results and the theoretical fit in the presence of the magnetic-resonance bottleneck indicates that, for Mg : Gd, substantial exchange narrowing of the fine-structure line has indeed occurred as stated in Sec. II. Further, the parameters used in the fit make it clear that fine structure can *never* be resolved in Mg : Gd. Breaking the bottleneck would only result in a substantial line broadening [see Fig. 1(b), where Δ_{eL} has been set equal to infinity], and not a resolution of fine-structure components. Thus, in materials with substantially larger exchange couplings, but probably comparable fine-structure splittings (e.g., Cu : Mn, Ag : Mn), there can be no hope of ever resolving the $S = \frac{5}{2}$ cubic-field fine structure. Measurements at temperatures lower than liquid helium do not help. The exchange relaxation rates would be reduced, but the higher S^z levels would depopulate and only the lowest-lying fine-structure line would be observed. Notwithstanding this dilemma, we have shown above that even unresolved fine structure can exhibit strong anisotropies in line position and width, from which the actual value of the fine-structure parameter can be extracted.

We suggest that unresolved fine structure may be the origin of the large "residual" width reported for Gd and Eu in a large class of powdered metallic alloys. The temperature dependence of an unresolved fine-structure spectrum in the intermediate-narrowed regime is such that a nar-

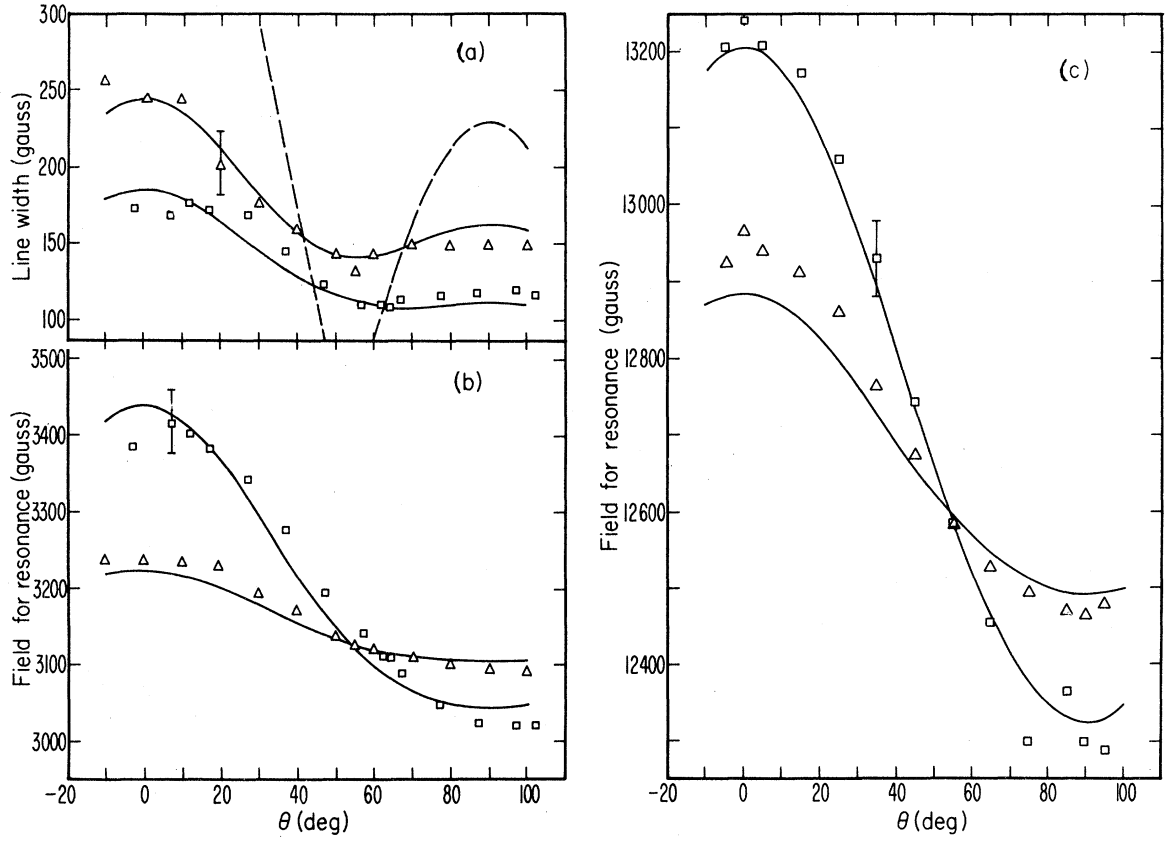

FIG. 3. (a) Linewidth as a function of the angle θ between the magnetic field and the c axis for Mg: Gd (400 ppm) at a frequency of 8.7 GHz. The squares indicate measurements at 1.4 °K; the triangles, 4.2 °K. The dashed line is the square root of the second moment, for $D=140$ G, at $T=1.4$ °K. The solid curves represent the theoretical values obtained from the fit of the resonance line shapes using the method of Barnes (Ref. 5). (b) Field for resonance as a function of angle for the same sample under the same conditions as in (a). (c) Field for resonance as a function of angle for the same sample as in (a), but at a frequency of 35 GHz. The squares indicate measurements at 1.6 °K; the triangles, 4.2 °K. The solid curves represent the theoretical values obtained from the same set of parameters as in (a) and (b), but at the higher frequency.

rowing occurs as the temperature is increased. This can be mistaken for evidence of a "dynamic" process, if only a simple molecular-field analysis is used. In addition to temperature-dependent residual widths, Fig. 3 also exhibits a temperature-dependent field for resonance caused by unresolved fine structure. While we are not implying that previous experimental interpretations of magnetic-resonance data on dilute Gd and Eu alloys are necessarily wrong, we suggest that some reexamination of these results using single-crystal samples might be in order, before peculiar temperature-dependent linewidths and shifts can be attributed unequivocally to dynamic factors.

Note added in proof. A calculation treating the problem of fine-structure narrowing in dilute magnetic alloys has also recently been performed by Plefka [Phys. Status Solidi b51 (to be published)] for $S=1$, and for general spin (unpublished). His results appear to be identical to those of Barnes, to second order in J, the order to which he worked.

ACKNOWLEDGMENT

We are indebted to Dr. Plefka for pointing out some errors in the Appendix, and for bringing to our attention the correct expression for the reduction of $1/T_2$ in the bottlenecked regime when the fine-structure lines can be resolved.

APPENDIX

The results of Barnes[5] for the dynamic transverse susceptibility of a dilute magnetic alloy can be written in collapsed form:

$$[\epsilon_{Sz}-\omega_0-i(\Delta^{Sz}_{Sz+1,\uparrow}+\Delta^{Sz}_{Sz+1,\downarrow}+\Delta^{Sz}_{Sz-1,\uparrow}+\Delta^{Sz}_{Sz-1,\downarrow})]\,\chi^{+-}_{Sz}(\omega_0)$$
$$+\sum_{Sz'\neq Sz}[i(\Delta^{Sz'}_{Sz,\uparrow}+\Delta^{Sz'}_{Sz,\downarrow})(\delta_{Sz,Sz'+1}+\delta_{Sz,Sz'-1})-\zeta_{Sz}]\,\chi^{+-}_{Sz'}(\omega_0)-\zeta_{Sz,e}\,\chi^{+-}_{e}(\omega_0)=\eta_{Sz}\,, \tag{A1}$$

$$(\epsilon_e-\omega_0)\,\chi^{+-}_e(\omega_0)-\sum_{Sz=-S}^{S-1}\zeta_{e,Sz}\,\chi^{+-}_{Sz}(\omega_0)=\eta_e\,,$$

where $\delta_{Sz,Sz'-1}$ is the Kronecker δ function. The expression (A1) is in the form of a set of coupled linear equations of dimension $2S+1$. This represents the manifold of the $2S$ fine-structure localized-moment resonance lines and the conduction-electron resonance line. The full response of the coupled system is given by

$$\chi^{+-}(\omega_0)=\sum_{Sz=-S}^{S-1}\chi^{+-}_{Sz}(\omega_0)+\chi^{+-}_e(\omega_0)\,, \tag{A2}$$

where the individual χ^{+-}_{Sz} and χ^{+-}_e are found from the solutions of (A1). The quantities appearing in (A1) are defined as follows, using the notation contained in the text of this paper:

$$\epsilon_{Sz}=\omega_{Sz}+\lambda(g_s/g_e)\,\chi_e\omega_e-i[\Delta_{Sz,e,\uparrow}+\Delta_{Sz,e,\downarrow}+\Delta_{SL}+\lambda(g_s/g_e)\,\chi^{(0)}_e(\Delta_{e,Sz}+\Delta^{Sz+1}_e-\Delta^{Sz}_e)]\,, \tag{A3}$$

$$\zeta_{Sz}=i\lambda(g_S/g_e)\,\chi^{(0)}_e(\Delta_{e,Sz}+\Delta^{Sz+1}_e-\Delta^{Sz}_e)\,, \tag{A4}$$

$$\zeta_{Sz,e}=\lambda\chi_{Sz}(g_S/g_e)\,\omega_e+i[-(g_S/g_e)(\Delta_{e,Sz}+\Delta^{Sz+1}_e-\Delta^{Sz}_e)-\lambda\chi^{(0)}_{Sz,\uparrow}(\Delta_{Sz,e,\uparrow}+\Delta^{Sz}_{Sz+1,\uparrow}+\Delta^{Sz}_{Sz-1,\uparrow})$$
$$-\lambda\chi^{(0)}_{Sz,\downarrow}(\Delta_{Sz,e,\downarrow}+\Delta^{Sz}_{Sz+1,\downarrow}+\Delta^{Sz}_{Sz-1,\downarrow})+\lambda\chi^{(0)}_{Sz+1,\uparrow}\Delta^{Sz+1}_{Sz,\uparrow}+\lambda\chi^{(0)}_{Sz+1,\downarrow}\Delta^{Sz+1}_{Sz,\downarrow}+\lambda\chi_{Sz-1,\uparrow}\Delta^{Sz-1}_{Sz,\uparrow}+\lambda\chi_{Sz-1,\downarrow}\Delta^{Sz-1}_{Sz,\downarrow}-\lambda\chi^{(0)}_{Sz}\Delta_{SL}]\,, \tag{A5}$$

$$\eta_{Sz}=\chi_{Sz}(g_s/g_e)\,\omega_e+i[(g_s/g_e)\,\chi^{(0)}_e(\Delta_{e,Sz}+\Delta^{Sz+1}_e-\Delta^{Sz}_e)-\chi^{(0)}_{Sz,\uparrow}(\Delta_{Sz,e,\uparrow}+\Delta^{Sz}_{Sz+1,\uparrow}+\Delta^{Sz}_{Sz-1,\uparrow})$$
$$-\chi^{(0)}_{Sz,\downarrow}(\Delta_{Sz,e,\downarrow}+\Delta^{Sz}_{Sz+1,\downarrow}+\Delta^{Sz}_{Sz-1,\downarrow})+\chi^{(0)}_{Sz+1,\uparrow}\Delta^{Sz}_{Sz,\uparrow}+\chi^{(0)}_{Sz+1,\downarrow}\Delta^{Sz+1}_{Sz,\downarrow}+\chi^{(0)}_{Sz-1,\uparrow}\Delta^{Sz-1}_{Sz,\uparrow}+\chi^{(0)}_{Sz-1,\downarrow}\Delta^{Sz-1}_{Sz,\downarrow}-\chi^{(0)}_{Sz}\Delta_{SL}]\,, \tag{A6}$$

$$\epsilon_e=\omega_e+\lambda\sum_{Sz=-S}^{S-1}\chi_{Sz}\,\omega_e-i[\Delta_{es}+\Delta_{eL}+\lambda(g_e/g_s)\sum_{Sz=-S}^{S-1}(\chi^{(0)}_{Sz,\uparrow}\Delta_{Sz,e,\uparrow}+\chi^{(0)}_{Sz,\downarrow}\Delta_{Sz,e,\downarrow})]\,, \tag{A7}$$

$$\zeta_{e,Sz}=\lambda\chi_e\,\omega_e-i[(g_e/g_s)(\Delta_{Sz,e,\uparrow}+\Delta_{Sz,e,\downarrow})+\lambda\chi^{(0)}_e(\Delta_{es}+\Delta_{eL})]\,, \tag{A8}$$

$$\eta_e=\chi_e\omega_e+i[-\chi^{(0)}_e(\Delta_{es}+\Delta_{eL})+(g_e/g_s)\sum_{Sz=-S}^{S-1}(\chi^{(0)}_{Sz,\uparrow}\Delta_{Sz,e,\uparrow}+\chi^{(0)}_{Sz,\downarrow}\Delta_{Sz,e\downarrow})]\,. \tag{A9}$$

The terms in (A3) and (A4) are defined by

$$\chi^{(0)}_{Sz}=[S(S+1)-S^z(S^z+1)]\,\frac{cg_s^2}{2}\,\frac{n_{Sz+1}-n_{Sz}}{\omega_{Sz}}\,,$$

$$\chi^{(0)}_{Sz,\uparrow}=\tfrac{1}{2}[S(S+1)-S^z(S^z+1)]\times\frac{cg_s^2}{Z_s}\,\frac{e^{-\beta(E_{Sz}+\omega_0)}-e^{-\beta E_{Sz+1}}}{\omega_{Sz}-\omega_0}\,,$$

$$\chi^{(0)}_{Sz,\downarrow}=\tfrac{1}{2}[S(S+1)-S^z(S^z+1)]\times\frac{cg_s^2}{Z_s}\,\frac{e^{-\beta E_{Sz}}-e^{-\beta(E_{Sz+1}-\omega_0)}}{\omega_{Sz}-\omega_0}\,,$$

$$\chi^{(0)}_e=\tfrac{1}{2}g^2_e\rho,\quad Z_s=\sum_{Sz=-S}^{S}e^{-\beta E_{Sz}},\quad n_{Sz}=e^{-\beta E_{Sz}}/Z_s,$$

$$\omega_S=(g_s/g_e)\,\omega_e,\quad \lambda=2J/g_eg_s\,.$$

In these expressions, E_{Sz} is the bare-Zeeman-plus-fine-structure energy of the localized spin level characterized by S^z and $\omega_{Sz}=E_{Sz+1}-E_{Sz}$. The enhanced susceptibilities are given by

$$\chi_{Sz}=\frac{\chi^{(0)}_{Sz}}{D}\left\{\frac{\omega_{Sz}}{\omega_S}+\lambda\,\chi^{(0)}_e\times\left[1+\lambda\left(\sum_{Sz'=-S}^{S-1}\frac{\omega_{Sz'}\,\chi^{(0)}_{Sz'}}{\omega_S}-\frac{\omega_{Sz}}{\omega_S}\sum_{Sz'=-S}^{S-1}\chi^{(0)}_{Sz'}\right)\right]\right\}\,,$$

$$\chi_e=\frac{\chi^{(0)}_e}{D}\left(1+\lambda\sum_{Sz=-S}^{S-1}\frac{\omega_{Sz}\,\chi^{(0)}_{Sz}}{\omega_S}\right)\,,$$

where

$$D=1-\lambda^2\chi^{(0)}_e\sum_{Sz'=-S}^{S-1}\chi^{(0)}_{Sz'}\,.$$

The relaxation terms appearing in Eqs. (A3)–(A9) are given by

$$\Delta_{Sz,e,\uparrow}=2\pi(\rho J)^2\times[(S^z+1)(\omega_0-\omega_{Sz})\,b^+(\omega_0-\omega_{Sz})-S^z\omega_0\,b^+(\omega_0)]\,,$$

$$\Delta_{Sz,e,\downarrow} = 2\pi(\rho J)^2 \times [S^z(\omega_0 - \omega_{Sz})\, b^-(\omega_0 - \omega_{Sz}) - (S^z+1)\,\omega_0 b^-(\omega_0)] \ ,$$

$$\Delta^{S^z+1}_{S^z,\uparrow} = \pi(\rho J)^2 [S(S+1) - S^z(S^z+1)]\,\omega_0 b^+(\omega_0) \ ,$$

$$\Delta^{S^z-1}_{S^z,\uparrow} = \pi(\rho J)^2 [S(S+1) - S^z(S^z+1)] \times (\omega_0 - \omega_{S^z-1} - \omega_{Sz})\, b^+(\omega_0 - \omega_{S^z-1} - \omega_{Sz}) \ ,$$

$$\Delta^{S^z-1}_{S^z,\downarrow} = -\pi(\rho J)^2 [S(S+1) - S^z(S^z+1)]\,\omega_0 b^-(\omega_0) \ ,$$

$$\Delta^{S^z+1}_{S^z,\downarrow} = -\pi(\rho J)^2 [S(S+1) - S^z(S^z+1)] \times (\omega_0 - \omega_{S^z+1} - \omega_{Sz})\, b^-(\omega_0 - \omega_{S^z+1} - \omega_{Sz}) \ ,$$

$$b^{\pm}(x) = (e^{\pm\beta x} - 1)^{-1} \ ,$$

$$\Delta_{e,Sz} = \pi c\rho J^2 \{2[(S^z+1)^2 n_{Sz+1} + S^{z2} n_{Sz}] + [S(S+1) - S^z(S^z+1)]\,[n_{Sz+1} + n_{Sz} + (n_{Sz+1} - n_{Sz}) \times \tanh(\tfrac{1}{2}\beta(\omega_S - \omega_0))]\} \ ,$$

$$\Delta_e^{Sz} = 2\pi c\rho J^2 S^z [S(S+1) - S^{z2}] n_{Sz} \ ,$$

$$\Delta_{es} = \sum_{S^z=-S}^{S-1} \Delta_{e,Sz} + \Delta_e^S - \Delta_e^{-S} \ .$$

The quantities Δ_{sL} and Δ_{eL} are the lattice relaxation rates for the localized and conduction-electron spins, respectively.

†Work supported in part by the National Science Foundation under Contract Nos. NSF GP-21290 and NSF GH-31973, and the U. S. Office of Naval Research, Contract No. N00014-69-A-0200-4032.

[1]L. J. Tao, D. Davidov, R. Orbach, D. Shaltiel, and C. R. Burr, Phys. Rev. Letters 26, 1438 (1971).
[2]E. P. Chock, R. Chui, D. Davidov, R. Orbach, D. Shaltiel, and L. J. Tao, Phys. Rev. Letters 27, 582 (1971).
[3]Y. Yafet, J. Appl. Phys. 39, 583 (1968).
[4]C. R. Burr and R. Orbach, Phys. Rev. Letters 19, 1133 (1967); see also C. R. Burr, thesis (University of California, Los Angeles, 1967) (unpublished).
[5]S. E. Barnes (unpublished).
[6]S. E. Barnes and J. Zitkova (unpublished).
[7]J. Zitkova, R. Orbach, and B. Giovannini, Phys. Rev. B 4, 4306 (1971).
[8]L. C. Hebel and C. P. Slichter, Phys. Rev. 113, 1504 (1959).
[9]A. W. Overhauser, Phys. Rev. 89, 689 (1953).
[10]H. Hasegawa, Progr. Theoret. Phys. (Kyoto) 21, 483 (1959).
[11]S. E. Barnes, J. Dupraz, and R. Orbach, J. Appl. Phys. 42, 1659 (1971); 42, 5908 (E) (1971).
[12]R. Chui and J. D. Riley (unpublished).
[13]R. Orbach and H. J. Spencer, Phys. Letters 26A, 457 (1968).
[14]I. Esterman, S. A. Friedberg, and J. E. Goldman, Phys. Rev. 87, 582 (1952); P. L. Smith, Phil. Mag. 46, 744 (1955); D. L. Martin, Proc. Phys. Soc. (London) 78, 1482 (1961).
[15]W. L. McMillan, Phys. Rev. 167, 331 (1967).
[16]T. Moriya, Progr. Theoret. Phys. (Kyoto) 28, 371 (1962); J. Phys. Soc. Japan 18, 516 (1963).
[17]E. R. Feher, Phys. Rev. 136, A145 (1964).

PHYSICAL REVIEW B VOLUME 6, NUMBER 7 1 OCTOBER 1972

Low-Temperature Transitions in Tetramethylammonium Manganese Chloride

B. W. Mangum and D. B. Utton
National Bureau of Standards, Washington, D.C. 20234
(Received 31 March 1972)

We have measured the proton nuclear magnetic resonance of tetramethylammonium manganese chloride, a linear chain antiferromagnet, in the temperature region 0.4–300 K. In addition, its ac magnetic susceptibility was measured in applied fields of 0 to 22 kG in the temperature range 0.3–4.2 K. When measured along the crystallographic c axis, the zero-field susceptibility had an anomaly at 0.84 K. When the external field was applied perpendicularly to the c axis below 0.8 K, a critical field of 11.5 kG was observed in dM/dB. The proton NMR did not indicate any *cooperative transition* to a magnetically ordered state of the Mn^{2+} spins. It did indicate, however, a gradual diminution of fluctuations in the crystallographic ab plane until a nonrandom order had been established between chains below approximately 0.8 K. We find that the tetramethylammonium groups cease all rotations below 39 K. In the region of 40 to 50 K, the tetramethylammonium groups not only undergo some hindered rotations, but their orientation is different from the published room-temperature x-ray diffraction results. Above 50 K only a single narrow NMR line is observed and, consequently, no additional information on the crystal structure could be obtained.

I. INTRODUCTION

There has been considerable interest recently in compounds whose magnetic properties approximate one-dimensional systems. Magnetic susceptibility,[1] electron-magnetic-resonance linewidths,[2] and neutron-scattering measurements[3,4] have shown $N(CH_3)_4MnCl_3$ to be a particularly good ex-